



Sodhro, A. H. , Gurtov, A. , Zahid, N. , Pirbhulal, S. , Wang, L. , Rahman, M. M. U. , Imran, M. A. and Abbasi, Q. H. (2020) Towards convergence of AI and IoT for energy efficient communication in smart homes. *IEEE Internet of Things Journal*, (doi: [10.1109/JIOT.2020.3023667](https://doi.org/10.1109/JIOT.2020.3023667))

The material cannot be used for any other purpose without further permission of the publisher and is for private use only.

There may be differences between this version and the published version. You are advised to consult the publisher's version if you wish to cite from it.

<http://eprints.gla.ac.uk/222671/>

Deposited on 28 August 2020

Enlighten – Research publications by members of the University of  
Glasgow

<http://eprints.gla.ac.uk>

# Towards Convergence of AI and IoT for Energy Efficient Communication in Smart Homes

Ali Hassan Sodhro, *Member, IEEE*, Andrei Gurtov, *Senior Member, IEEE*, Noman Zahid, Sandeep Pirbhulal, Lei Wang, Muhammad Mahboob Ur Rahman Muhammad Ali Imran, *Senior Member, IEEE*, Qammer H. Abbasi, *Senior Member, IEEE*

**Abstract**—The convergence of Artificial Intelligence (AI) and Internet of Things (IoT) promotes the energy efficient communication in smart homes. Quality of Service (QoS) optimization during video streaming through wireless micro medical devices (WMMD) in smart healthcare homes is the main purpose of this research. This paper contributes in four distinct ways. First, to propose a novel Lazy Video Transmission Algorithm (LVTA). Second, a novel Video Transmission Rate Control Algorithm (VTRCA) is proposed. Third, a novel cloud-based video transmission framework is developed. Fourth, the relationship between buffer size and performance indicators i.e., peak-to-mean ratio (PMR), energy (i.e., encoding and transmission) and standard deviation is investigated while comparing the LVTA, VTRCA, and Baseline approaches. Experimental results demonstrate that the reduction in encoding (32%, 35.4%) and transmission (37%, 39%) energy drains, PMR (5, 4), and standard deviation (3dB, 4dB) for VTRCA and LVTA, respectively, is greater than that obtained by Baseline during video streaming through WMMD.

**Index Terms**—Energy efficient communication, Smart Homes, Convergence AI, IoT, Video Streaming, Wireless Micro Medical Devices, LVTA, VTRCA, Cloud-based

## I. INTRODUCTION

THE convergence of Artificial Intelligence (AI) and Internet of Things (IoT) empowers energy efficient communication in smart homes. The multimedia is the best source to the attention from every corner to entertain

Ali Hassan Sodhro is with Computer and Information Science Department, Linköping University, Linköping, Sweden and Sukkur IBA University, Sukkur, Sindh, Pakistan, E-mail: ali.hassan.sodhro@liu.se

Andrei Gurtov is with Computer and Information Science department, Linköping University, Linköping, Sweden, E-mail: andrei.gurtov@liu.se

Noman Zahid is with Sukkur IBA University, Sukkur, Sindh, Pakistan, Email: noman.mece17@iba-suk.edu.pk

Sandeep Pirbhulal is with the Universidade da Beira Interior, Portugal, E-mail: sandeep.hemnani28@gmail.com

Lei Wang is with the Shenzhen Institutes of Advanced Technology, Chinese Academy of Sciences, Shenzhen, China, Email: wang.lei@siat.ac.cn

Muhammad Mahboob Ur Rahman is with the Electrical Engineering Department, Information Technology University, Lahore, Pakistan, Email: mahboob.rahman@itu.edu.pk

Muhammad Ali Imran is with the School of Engineering, University of Glasgow, UK, E-mail: muhammad.imran@glasgow.ac.uk

Qammer H. Abbasi is with School of Engineering, University of Glasgow, UK, E-mail: qammer.abbasi@glasgow.ac.uk

the needs of everyone at any time over joint AI and IoT networks with high data rates and lower latency. Wireless micro medical devices (WMMDs) are the leading players for portraying the detailed features of a desired application [1].

The proliferation in innovative, advanced and cost-effective wireless micro devices equipped with sensors, such as complementary metal oxide semiconductor (CMOS) camera and sensor networks have become the center of attention from both academia and industry perspectives. It is vital to optimize the quality of service (QoS) during video transmission through WMMDs. It is supposed to sense, retrieve, store, process, transmit, and communicate information from a source node to a destination node as shown in Fig.1. The sensor-enabled systems for video transmission can monitor a diverse range of applications, such as surveillance, emergency response (e.g., fire-fighting), military, transportation systems, smart cities, and healthcare, among others [2], [3].

In addition, these systems have the capability to integrate with other technologies to provide proper guideline or relevant real-time based platforms [4], [5]. Many researchers have raised the questions and explored the challenges faced by multimedia sensor networks, but still there is a considerable room for improvement by investigating appropriate solutions for optimizing QoS during video transmission through sensor-driven WMMDs [6].

It is predicted from the CISCO service provider team that media, especially video, streaming plays a prominent role in the current technological era with significant traffic contribution of up to 60% and this is expected to reach up to 80% by the end of 2019 [3]. This paper focuses on cloud-based deployment, QoS optimization and interpretation while transmitting video through WMMDs.

Fig.1 reveals the proposed video transmission through WMMD framework which consists of media streaming server which stores pre-recorded encoded VBR video of Medical-education for elderly people and infants, video sensor nodes; which captures, processes and transmits multimedia contents in real time, base station (BS) which decodes video, gateway video sensor, sender, and

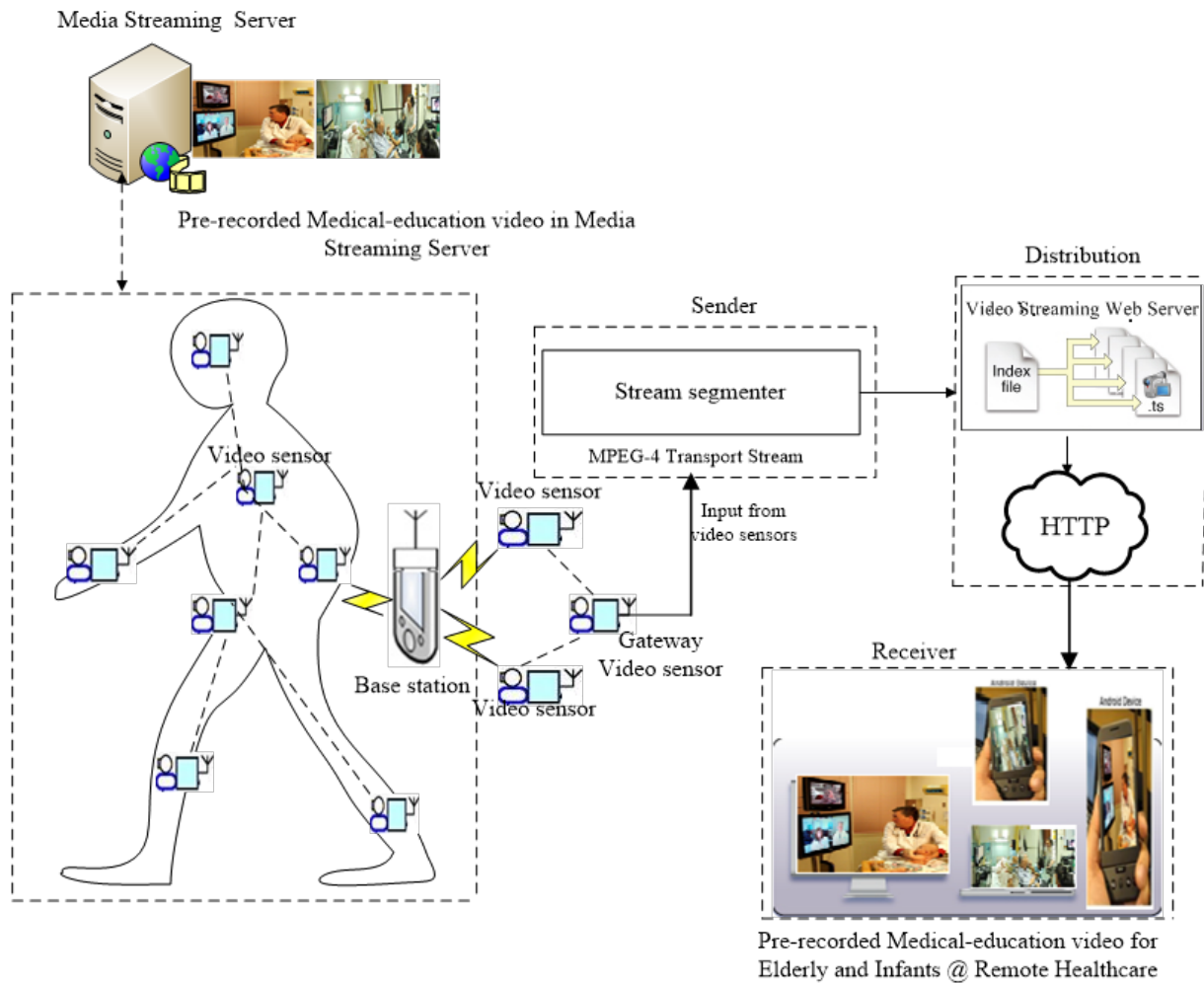


Fig. 1. Cloud-based framework of efficient video transmission through wireless micro medical devices

receiver. A single hop communication with a simple star network topology is considered for transmission of video-on-demand from media streaming server. The media streaming server provides channel content and transmits at the rate of 30 frames per sec to video sensor nodes on human body. The WMMD on human body capture the pre-recorded video from media streaming server through built-in cameras and forward that video to the BS where video is decoded and then transferred to the gateway video sensor node.

Finally, the decoded video is distributed and transmitted through internet (IP network) which is connected with the hospital monitoring network and intended receiver as shown in Fig.1. In this paper, we make the following contributions:

- devising a Lazy Video Transmission Algorithm (LVTA),
- proposing a Video Transmission Rate Control Al-

gorithm (VTRCA),

- developing an energy efficient cloud-based framework for video transmission through sensor-enabled WMMMD nodes,
- establishing a relationship between buffer size and performance indicators, particularly encoding and transmission energy consumption, PMR, and Std.dev.
- evaluating and comparing the performance of the proposed LVTA and VTRCA algorithms against Baseline.

The remaining of this paper is structured as follows. Existing research works are presented in Section II. QoS optimization algorithms for video transmission are developed in Section III. Section IV discusses encoding and transmission energy drains. Experimental results and discussion are presented in Section V. Section VI, concludes this paper with emerging future directions

## II. RELATED WORKS

In [1], a detailed survey highlighting the innovative and emerging technological trends and practices is presented [2]. Latest and emerging network generation is expected to bring a paradigm shift in the delivery of a voluminous of media content at remote locations [3]. Remarkable and self-aware technologies are the cornerstone for every domain with the help of Internet of things (IoT)-based trends [4], [5], but QoS optimization during media transmission is not focused. Transmission power control-driven energy optimization schemes during human vital sign signals (i.e., electrocardiogram (ECG) and images) delivery to remote hospitals are proposed in [6], [7], [8].

The IoT, bigdata, their interconnection to real-time issues, consequences, and future challenges are highlighted in [7], but QoS optimization during multimedia streaming is not discussed. A detailed survey about communication strategies, techniques, frameworks, and channel modeling for healthcare are addressed in [?] [9]. The IoT-driven technologies are discussed in detail to promote green and sustainable world, but QoS is not the key entity being focused [10]. Hybrid WMMD and IoT mechanism is proposed to effectively allocate resources (i.e., power and battery lifetime) in sensor-based healthcare [11], but QoS during multimedia transmission is not focused.

The human physiological signals are transmitted to examine the healthcare of elderly patients by developing an energy optimization model [12] [13], [14]. In [15], packet transmission strategies are proposed for energy and battery life management for healthcare applications, but QoS optimization is not highlighted. Layered approach for energy optimization during media transmission is designed by [16].

The power-aware techniques and frameworks are developed for joint IoT and BSN platform in medical world [17], [?] to promote the economical and sustainable healthcare platform. In [18], [19], [20] and [?], [21], a healthcare platform for remote patients with better services is designed, but QoS optimization during video transmission through WMMD is not focus of these papers. Authors in [7] develop mechanism for ultradense IoT networks to energy aware computation and transmit power allocation. The [22] design an intelligent energy efficiency technique for lightweight portable devices.

Authors in [23], [24] describes the smart home and smart cities applications with the existing challenges, recommendations and different solutions by the integration of latest technology, i.e., IoT, 5G. AAI. Long et al [25] designed an edge computing framework for the multimedia IoT systems to avoid the congestion and delays which large size video chunks faces on the long distance transmission.

In [26], [27], [7], fair resource allocation techniques are presented for ad-hoc networks, smart cities and healthcare fields. The aforementioned research contributions have highlighted the emerging role of sensor networks, IoT, power-aware, and sustainable pervasive healthcare [20]. Nevertheless, QoS optimization has not been the main focus during medical media transmission. Only [6] and [9] investigated energy optimization techniques by adopting real-time video datasets [14]. Moreover, energy (i.e., encoding and transmission) drain and network performance analysis, impact of client buffer size, PMR, and high peak rates during video transmission in WMMD are not addressed.

## III. PROPOSED VIDEO TRANSMISSION ALGORITHMS FOR WIRELESS MICRO MEDICAL DEVICES

This section proposes VTRCA and LVTA for QoS optimization during video transmission through WMMDs.

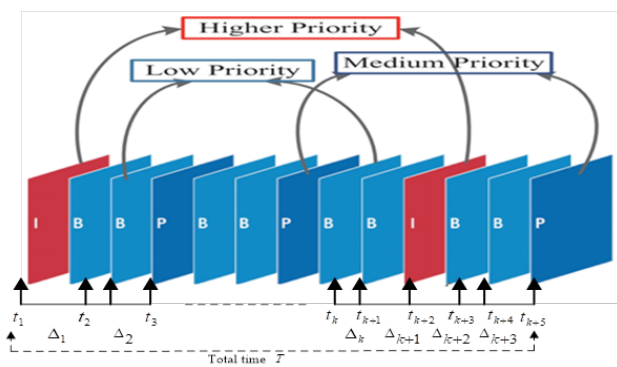


Fig. 2. Video frames arrival with elapsed time period.

In video, there are three main frame types: inter-coded (I), bi-directional (B), and previous (P). Among these, I-frame is given the top-most priority due to its remarkable role during operation, P-frame is assigned the medium level, and B-frame is given the lowest priority in a video sequence during communication as shown in Fig. 2. Each frame is allocated with a time slot  $t$ , while  $\Delta$  and  $T$  show the time between frames and the entire video time, respectively. In our system, two nodes (i.e., the transmitter and receiver (i.e., BS) nodes) are adopted for video transmission through WMMD nodes.

There are eight main components of media transmission: video frames  $VF$ , buffer size  $Buffer$ , initial elapsed time between frames  $t_o$ , average video frames received at receiver  $B(t)$  at  $[1,t]$  interval without buffer overflow, frame rate  $r(t)$  at receiver, initial buffer size  $q\_buffer$ , the total length of video frames  $L\_vf(t)$  at  $t=1, \dots, VF$ , video frame rates with the maximum value being  $R\_max$ , the minimum value being  $R\_min$ , and

the average value being  $R_{avg}$ , as well as the average video frame size consumed at receiver or base station, specifically  $D(t)$ . Media transmission mechanism through WMMD nodes is presented in Figs. 1 and 2.

$$\Delta_k = t_{k+1} - t_k \quad (1)$$

whereby  $\Delta_k$  and represent the inter-arrival period of each frame, and the total time of the video stream, respectively, as shown in Eqs. (1) and (2), which explain the total video time and length of video streams, respectively

$$\sum_{i=1}^{VF} \Delta_i = T \quad (2)$$

$$\begin{aligned} L_{vf}(1) &= Vf_1 & Vf_2 & & Vf_3 \\ L_{vf}(2) &= Vf_4 & Vf_5 & & Vf_6 \\ L_{vf}(3) &= Vf_7 & Vf_8 & & Vf_9 \\ \dots &= \dots & \dots & & \dots \\ \dots &= \dots & \dots & & \dots \\ L_{vf}(480) &= Vf_{1438} & Vf_{1439} & & Vf_{1440} \end{aligned} \quad (3)$$

#### A. Lazy Video Transmission Algorithm

With a large startup delay, more energy is saved by Lazy Video Transmission Algorithm (LVTA) by arranging the video frames  $= \{vf_1, vf_2, \dots, vf_{n-1}, t\}$  in an ON-OFF manner at frame rate  $r(t)$ , client buffer size, and initial delay time  $t_o$ . Eq.(4) reveals that total video length is the sum of individual video frame length.

$$L_{vf}(i) = \sum_{i=1}^{VF} vf_i \quad (4)$$

where  $L_{vf}$  and  $vf_i$  are the video frame length and the frame, respectively. Eq.(6), tells that average video length is the sum of all the video streams with random rate and size.

$$D(t) = \sum_{i=1}^{VF} vf_i \quad (5)$$

Similarly,  $D(k)$  and  $vf_k$  at  $k \geq 0$ , represent the aggregate frame size of  $k$ th video frame and the  $i$ th frame, respectively. Besides, if  $\sum L_{vf_{k+1}} - L_{vf_k} \leq r \times t$ , then  $\sum L_{vf_k} = D(k)$  at  $k = 1, \dots, VF$ . The feasible video transmission mechanism  $\gamma_{LVTA} = \{r; t_o, t_1, t_2, \dots, t_{2n+1}\}$  with frame rate  $r$  and the number of ON and OFF states in LVTA is presented in Fig. 4. When video is transmitted to BS very late, the minimum required *Buffer* and  $t_o$  can be obtained in an ON-OFF manner as represented in Eq. (8) and Fig. 3 and 4. LVTA computes the function  $\gamma_{LVTA}(t)$  for obtaining  $\gamma_{LVTA}(kt) = L_{vf_k}$  and hence the suitable video transmission schedule. Moreover,  $\gamma_{LVTA}$  contains few horizon sections with OFF transmission states for

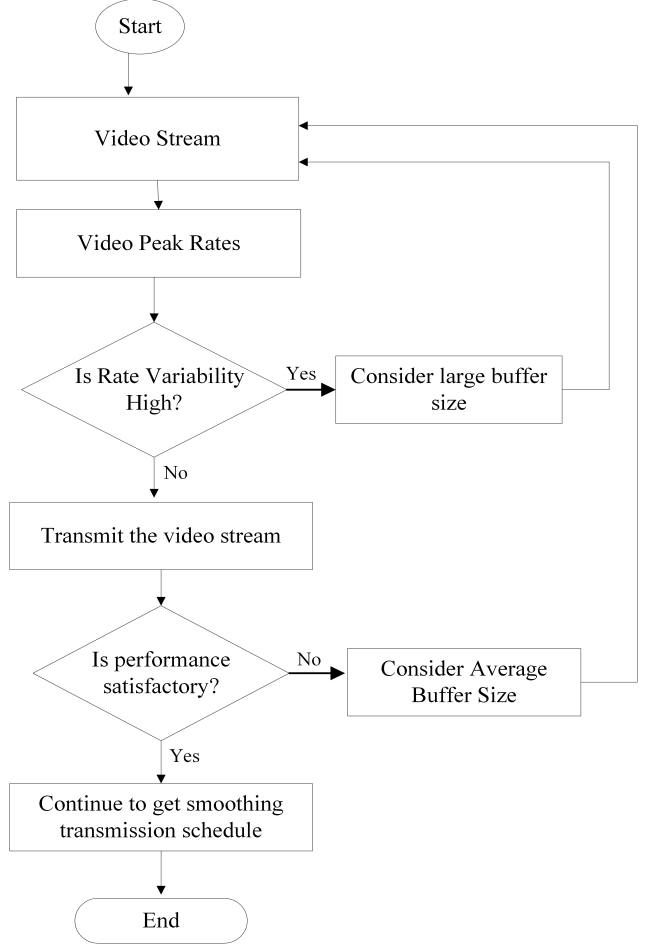


Fig. 3. Flowchart of the Lazy Video Transmission Algorithm

using small *Buffer*. Here,  $\Delta_k$  and  $t_k$  represent inter-arrival and time of each frame, respectively; see Fig 2 as well as Eqs. (3) and (4).

**Theorem 1:**  $Buffer_{VF}(r) = \max_{k=0}^{VF} \{\sum L_{vf_k} - D(k-1)\}$  reveals the acceptable buffer size for initial frame rate  $r$ .

$$\begin{aligned} L_{vf_i}(1) &= \sum_{i=1}^{VF} vf_i \quad \forall i \geq VF - 1 \\ L_{vf_k} &= \max\{D(k), \sum_{k=1}^{VF} vf_k - r \times t\} \quad \forall 0 \leq k < VF - 1 \end{aligned} \quad (6)$$

$$\gamma_{LVTA}(t) = \begin{cases} r, & t \in (t_{2i}, t_{2(i+1)}) \\ 0, & otherwise \end{cases} \quad (7)$$

More encoding and transmission energies are depleted while transmitting a raw video with high peak rates and rate variability (i.e., Std dev), so the proposed LVTA first changes the video stream into equal frame intervals with processing time interval of  $[0, T]$ . After adopting

LVTa, an efficient video transmission schedule can be achieved. The aggregated transmission function  $\Gamma(t)$  is the combination of  $\gamma_{LVTa}(t)$ , i.e.,  $\Gamma(t) = \int_{-\infty}^t \gamma(x)dx$ . This can also be represented as  $\gamma(kt) = \Gamma k$ . Due to the ON-OFF nature of  $\gamma_{LVTa}$ , video frames are transmitted in a slow fashion, which saves energy even at smaller  $Buffer_{VF, \gamma_{LVTa}}$  as shown in algorithm and Eqs. (7) and 8).

**Inputs:**  $r, VF, L_{vf}, Buffer$

**Output:** *Qos Optimization, Average Video Transmission Schedule*

$$\sum_{i=1}^{VF} v_{f_i} = L_{vf_i} \quad \forall i \geq VF - 1$$

$$\sum_{i=1}^{VF} L_{vf_k} = \max\{D(k), \sum_{k=1}^{VF} v_{f_k} - r \times t\} \quad \forall 0 \leq k \leq VF - 1$$

$$t_o = -L_{vf_i} / r$$

$$j = 1$$

for

$$k=0 \rightarrow VF - 1$$

do

begin

if

$$\sum_{k=1}^{VF} L_{vf_{k+1}} - L_{vf_k} \leq r \times t$$

begin

$$t_j = L_{vf_k}$$

$$t_{j+1} = L_{vf_{k+1}} - (L_{vf_{k+1}} - L_{vf_k}) / r$$

$$j=j+2$$

end

end

end

**Proof:** As from theorem 1,  $Buffer_{VF}(r) = \max_{k=0}^{VF} \{\sum L_{vf_k} - D(k - 1)\}$ . Assume that  $i, 0 \leq i \leq VF$ , during which  $\sum_{i=1}^{VF} v_{f_i} - D(i - 1) = Buffer_{VF, \gamma_{LVTa}}$ . It is assumed that  $\gamma'_{LVTa}$  needs minimum buffer  $Buffer_{VF, \gamma'_{LVTa}}$  unlike  $\gamma_{LVTa}$  for transmitting video content  $VF$ . Thus  $\Gamma' \leq \sum L_{vf_i}$  and formulates two main related cases as below. **Case 1:** If  $\sum L_{vf_{k+1}} - L_{vf_k} \leq r \times t$ , we have  $\sum L_{vf_i} = D(i)$ . Since,  $\Gamma' \leq \sum L_{vf_i}$ , it contradicts the feasibility condition for  $\gamma'_{LVTa}$ .

**Case 2:** Otherwise,  $\sum L_{vf_{k+1}} - L_{vf_k} \approx r \times t$ . Assume  $i'$  is the integer with value greater than  $i (i' > i)$ , while  $\sum L_{vf_{i'+1}} - L_{vf_{i'}} \leq r \times t$  when  $\sum L_{vf_{i'}} = D(i')$ , which leads to  $\Gamma'_i \leq \Gamma'_{i'} + (i' - i)t \leq \sum L_{vf_{i'}} + (i' - i)t = \sum L_{vf_{i'}} = D(i')$ , and this is not the optional status of  $\gamma'_{LVTa}$ . Thus it can be said that  $Buffer_{VF, \gamma'_{LVTa}}$  of  $\gamma'_{LVTa}$  is smaller. Small buffer size is sufficient for  $\gamma'_{LVTa}$  to transmit the video through

WMMD. Furthermore, it can be said that  $\gamma_{LVTa}$  is the feasible transmission schedule for transmitting entire video. Hence, for  $\gamma_{LVTa}$ , mathematical representation of transmission function  $\Gamma(t)$  can be written as  $\Gamma(kt) \geq \sum L_{vf_k}, \forall 0 \leq k \leq VF - 1$ .

Furthermore, at starting delay time  $t_o = 0$  and some video frames  $L_{vf_i}$  are stored in the buffer as  $Buffer_{VF, \gamma_{LVTa}}$ , which predict the future longer playbacks. It is observed that LVTa reduces rate variability of video sequence due to its ON-OFF nature.

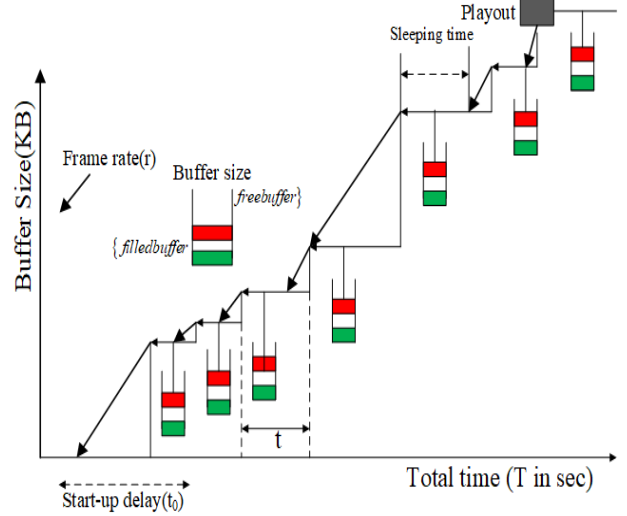


Fig. 4. Video Transmission Schedule of Lazy Video Transmission Algorithm.

## B. Video Transmission Rate Control Algorithm

The proposed VTRCA manages the high peak variable frame rate of video sequence  $VF$  and operation time of WMMD. A discrete video frame model is adopted  $t \in \{1, 2, \dots, VF\}$ , in which  $VF$  is taken from the receiver's (i.e., base station) buffer size, and frame rate of  $r(t)$ . The constant  $Buffer, B(t) = \min\{D(t - 1) + Buffer, D(VF)\}$  for  $t = 2, \dots, VF$ , with  $Buffer(1) = Buffer$  and  $Buffer(0) = 0$  can be achieved. To remedy the abundance and starvation ( $R_{min} \leq R_{avg} \leq R_{max}$ ), it is necessary to propose an optimal transmission pattern by considering real-time vector, such as  $Q = [a(1), \dots, a(VF)]$  as presented in Fig. 5 and 6. VTRCA is the potential candidate in optimizing the QoS by adapting the  $Buffer$  during video transmission. For minimum energy drain, it is vital to adopt the video frame rate  $[R_{max}, R_{min}]$ , because optimal video transmission rate  $R_{avg}$  minimizes the energy dissipation by delivering video sequence at bounded level. If  $R_{avg}$  is larger than  $R_{max}$ ,  $VF$  must be transmitted at  $R_{max}$  to reduce  $Buffer$  overflow. Similarly, at  $R_{avg}$  less than  $R_{min}$  video frame rate will be  $R_{min}$  to

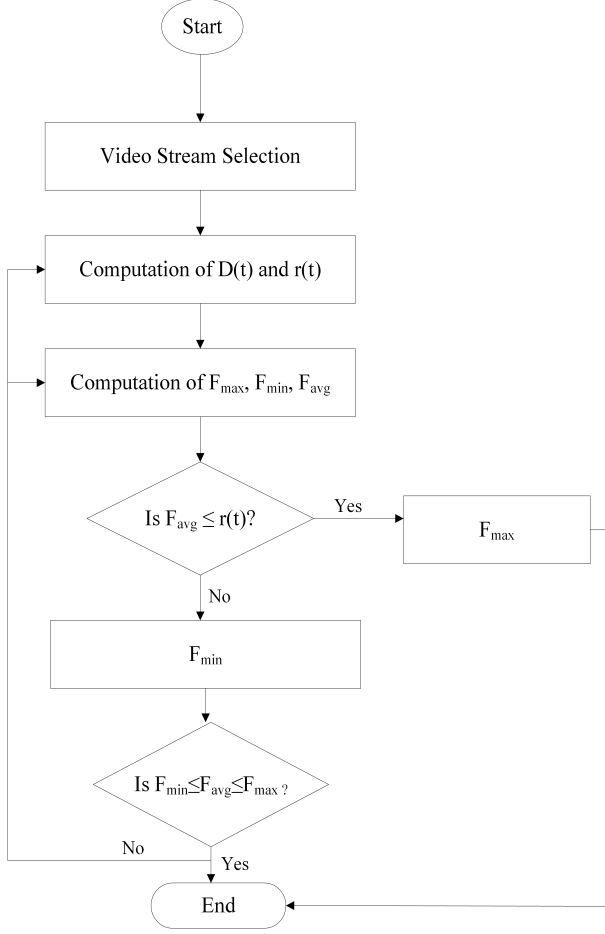


Fig. 5. Flowchart of Video Transmission Rate Control Algorithm

minimize *Buffer* starvation. Therefore, it can be predicted that energy is optimized at the optimal *Buffer* flow. Here,  $R_{max}$  depicts the maximum transmission rate of video frames without *Buffer* overflow as presented in Eq. (9).

**Inputs:** Data rate and total number of video frames,  $VF$ ,  $t_B$ ,  $t_D$ ,  $L_{vf}$ , *Buffer*

**Output:** Qos Optimization, Average Video Transmission Schedule  
for

$t=0 \rightarrow VF - 1$

do

begin

if

$F_{avg}(VF) \leq r(t)$

begin

$F_{max} = \frac{\sum_{t=1}^{VF} D(t) + Buffer}{t_B}$

if

$F_{avg} = \frac{F_{min} + F_{max}}{2}$

end

end

$$R_{max} = \frac{\sum_{t=1}^{VF} D(t) + Buffer}{t_B} \quad (8)$$

$$t_B = \frac{B(t) - q\_buffer}{t} \quad (9)$$

$$R_{min} = \frac{\sum_{t=1}^{VF} D(t) - q\_buffer}{t_D} \quad (10)$$

$$t_D = \frac{D(t) - q\_buffer}{t} \quad (11)$$

$$R_{avg} = \frac{R_{max} + R_{min}}{2} \quad (12)$$

Here,  $t_B$  exhibits the starting time when **Buffer** size is completely loaded, by supporting transmitter node to deliver data at  $R_{max}$  and  $R_{min}$  for minimizing under-flow and overflow of *Buffer*. While  $t_D$  reveals the time period at which *Buffer* is totally empty. Feasible and efficient media transmission schedule can be achieved at the condition  $R_{min} \leq R_{avg} \leq R_{max}$ . VTRCA remarkably contributes in obtaining an efficient video transmission by avoiding large peak rates, and Std. dev, hence, the encoding and transmission energy is drained ( $1.3 \leq \gamma \leq 2$ ) as presented in Fig. 6 and 7.

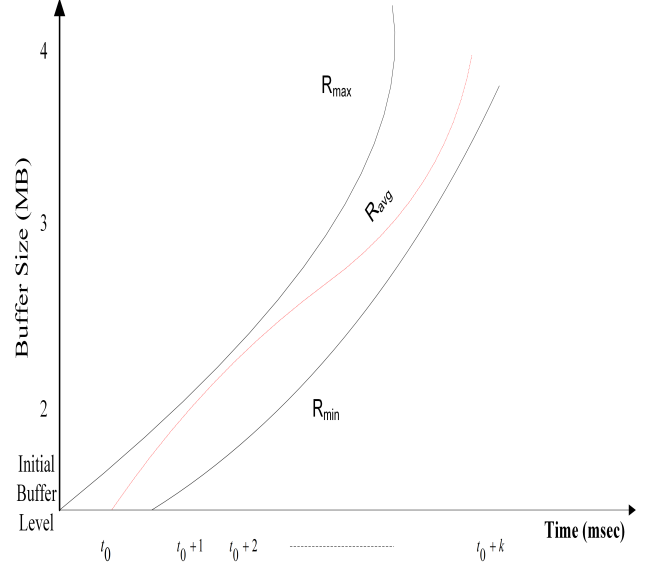


Fig. 6. Optimal schedule of Video Transmission Rate Control Algorithm

#### IV. ENCODING AND TRANSMISSION ENERGY CONSUMPTION DURING VIDEO STREAMING

Due to the stored nature of the video, camera's energy dissipation is not included into our test-bed, hence, only transmission of video sequence is performed through

wireless link. Thus, total energy is the sum of both encoding and transmission energy drains. Fig. 7 shows that average encoding energy consumption  $E_{enc_{avg}}$  decreases as data rate increases. On the other hand the transmission energy consumption  $E_{tx}$  is directly proportional to data rate. Generally, the speed of CPU is characterized by clock frequency  $f$ , which is linearly proportional to the supply voltage  $V$ . For instance, in a Motorola CMOS 6805 microcontroller, there are several distinct pair connections between two important ingredients (i.e., voltage and frequency, particularly 6 MHz at 5.0 Volts, 4.5 MHz at 3.3 Volts, and 3 MHz at 2.2 Volts) etc.

It reveals a direct and proximity between voltage and clock frequency, and clearly shows that the encoding power consumption per cycle  $P_{enc}$  is proportional to voltage square  $V^2$ . Therefore, by decreasing supply voltage  $V$ , charging and discharging time increases, and hence the lower the frequency will be. The average encoding power consumption rate of CPU is given by Eq. (13):

$$P_{enc} = k \times C \times V^2 \times f \quad (13)$$

Here,  $K$ ,  $C$ , and  $f$  are the proportionality constant, capacitance of the circuit, and the CPU frequency respectively. The circuit delay  $t_{deay}$ , which determines the possible maximum clock frequency  $f$  is dependent on  $V$  as shown in Eq. (14)

$$t_{deay} \propto f^{-1} \propto \frac{V}{(V-V_{th})^\gamma}$$

or simply we can write it as shown below:

$$f \propto \frac{(V - V_{th})^\gamma}{V} \quad (14)$$

Here,  $V_{th}$  is the threshold voltage of CMOS circuit and  $\gamma$  is the velocity saturation index. Thus, in this condition when  $\gamma$  is equal to 2 and  $V = V_{th}$ , then  $f \propto V^{(\gamma-1)}$ . Therefore, eq. (17) can be replaced by Eq. (18).

$$P_{enc} = K \times C \times V^3 = V \times V^2 \quad (15)$$

In Equation (15), constants ( $K = C = 1$ ). Most of the time, energy depletion is minimized by slowing down the processor's speed, that is why higher values of voltage  $V^2$  is not considered because reduction in CPU voltage minimizes encoding energy drain substantially due to linear connection between encoding energy and voltage (i.e.,  $E_{enc} \propto V^2$ ). Thus, Eq. (15) can be modified as Eq. (16), whereas (4.95V),  $I$ , and  $t_{enc}$  represent the voltage, current flow, and the time taken by the WMMD, respectively, while encoding a video. Encoding a single frame to MPEG-4 takes around 4ms.

$$E_{enc} = P_{enc} \times t_{enc} = V \times I \times t_{enc} \quad (16)$$

Actual energy depletion per-cycle count can be obtained from the data sheet of the corresponding processor, based

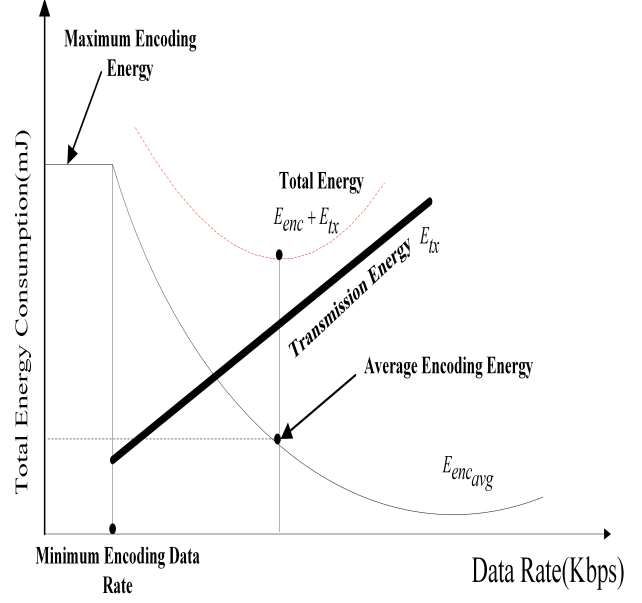


Fig. 7. Relationship between Data Rate and Total Energy Consumption

TABLE I  
EXPERIMENTAL ATTRIBUTES

Parameter	Value
Number of frames	1440
frame rate (r(t))	3 per sec
Frame arrival time (t)	5msec
Buffer Size	0.064MB,0.512MB,2MB,4MB
Voltage	4.5 V
Total time (T)	8 minutes
Frame length ( $L_{vf}$ )	100 Bytes
Inter-frame time ( $\Delta$ )	1 msec
Starting buffer size	0
Initial current (I)	200 mA

on WMMD, and their energy consumption per-cycle value of 1.215nJ is adopted in our experimental setup. Several components are contributing to the total energy drain, such as average cycles per instructions (CPI). Another component is the instruction count (IC), which represents the total number of instructions to encode a video stream. Thus, the average encoding energy dissipation can be estimated by inserting Eq. (16) into Eq. (17).

TABLE II  
QoS OPTIMIZATION DURING VIDEO TRANSMISSION

Video Stream from WMMD		PMR (%)	Std.dev of frame inter-arrival (dB)	Encoding Energy Consumption[J]		Transmission Energy Consumption[J]	
				inter-coding	intra-coding	inter-coding	intra-coding
Buffer Size=0.064 MB	Baseline	5.52	11.8	81.43	85.09	79.09	84.25
	LVTA	1.94	5.53	54.0	55.69	56.95	65.01
	VTRCA	1.81	4.25	57.65	59.95	52.05	60.23
Buffer Size=0.512 MB	LVTA	1.77	4.12	62.87	64.67	63.33	70.79
	VTRCA	1.46	3.75	63.85	65.38	63.01	67.13
Buffer Size= 2 MB	LVTA	1.58	3.21	70.11	74.45	68.56	76.89
	VTRCA	1.33	2.64	68.09	73.73	66.50	78.0
Buffer Size= 4 MB	LVTA	1.48	2.27	76.35	78.0	73.0	80.35
	VTRCA	1.15	1.85	72.90	76.03	67.19	79.11

$$E_{enc_{avg}} = \frac{IC \times CPI \times E_{enc}}{VF} \quad (17)$$

In Equation 18,  $E_{enc}$  is the encoding energy of each video. The total energy dissipation is the combination of transmission and encoding energy during media transmission as shown in Fig 9. The average video encoding energy is calculated using Eq. (18). Energy consumed for a transmission of the encoded  $VF$  is computed by using Eq. (18).

$$E_{tx} = V \times I \times t_{tx} \quad (18)$$

To transmit at frequency 2.4 GHz and transmission power of 0dBm, then sensor node with integrated CC2420 transceiver draws a current of 17mA. Finally,  $t_{tx}$  is the transmission time of the sensor node. We chose video frame length  $L_{vf}$  of size 100 bytes and initial current value of 200mA.

## V. EXPERIMENTAL RESULTS AND DISCUSSION

A test-bed is established by considering a real-time video recorded and encoded by the WMMD and MPEG-4 encoder (640x480) [15]. VTRCA and LVTA are proposed for QoS optimization in terms of energy (i.e., encoding, transmission), PMR, Std.dev by adopting initial delay  $t_0$  and buffer size. Detailed parameters for supporting Monte Carlo process is adopted as shown in Table 1. Moreover, Table 2 and Fig. 8 reveal that the proposed VTRCA optimizes QoS better than the Baseline and LVTA in terms of energy (i.e., encoding and transmission), PMR, and Std.dev; in-line with different client buffer sizes.

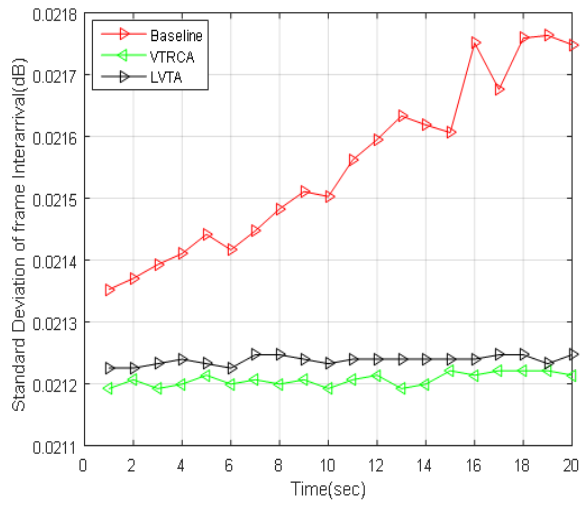
The Fig. 8(a), (b), reveal the trade-off between QoS metrics such as Std.dev, PMR and time. Fig. 8(c), shows the relationship between delay and buffer size to analyze the QoS performance of Baseline, LVTA and VTRCA with low, average and high rate accordingly. The VTRCA saves encoding and transmission energy of (37%, 39%), and minimizes PMR of 5 Std dev of 4dB, consequently. While VTRCA optimizes encoding, transmission energy of (32%, 35.4%), with PMR of 4, Std.dev of 3dB respectively, when compared to the Baseline.

Fig.9 (a) illustrates the trade-off between frame index and PSNR for proposed VTRCA, LVTA and Baseline. It is found that VTRCA has higher PSNR than LVTA and Baseline, and Baseline shows less PSNR, while LVTA reveals in-between the VTRCA and Baseline from point view of this performance metric. The trade-off between charge optimization and number of sensor nodes for measuring battery capacity and impact on its lifetime is drawn in Fig.9 (b) for proposed VTRCA, LVTA and Baseline. It is analyzed that VTRCA outperforms the LVTA and Baseline during video transmission through WMMD, while Baseline consumes more battery charge than both LVTA and VTRCA.

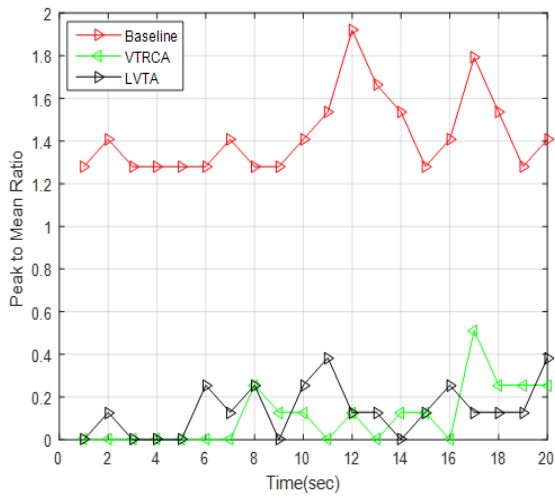
Finally, Fig.9 (c) presents the relationship between modulation level and total energy drain (encoding and transmission) for proposed VTRCA, LVTA and Baseline. In this case LVTA outperforms the VTRCA and Baseline, while VTRCA shows less energy dissipation than Baseline.

## VI. CONCLUSION

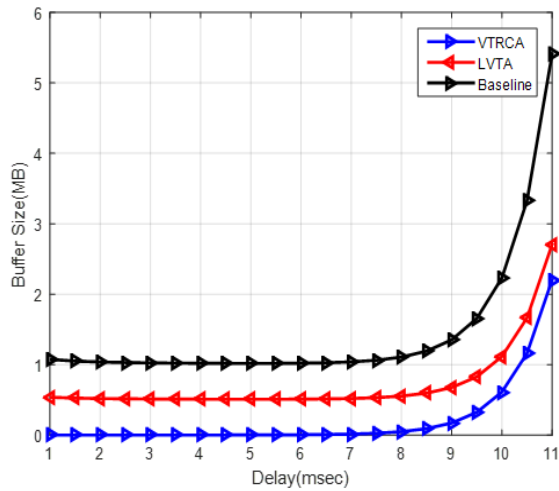
The coordination between AI and IoT empowers the efficient communication in smart healthcare homes. Due



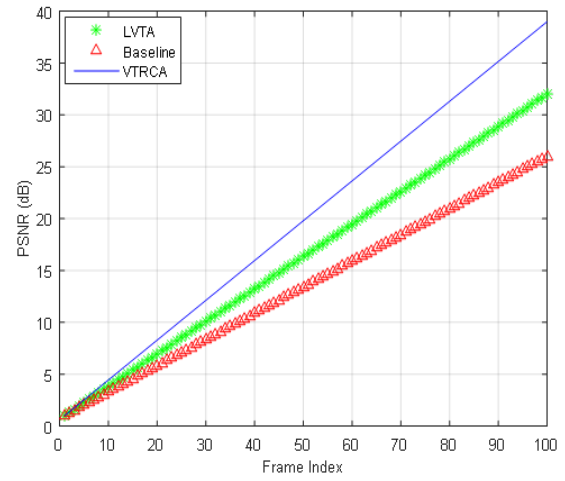
(a)



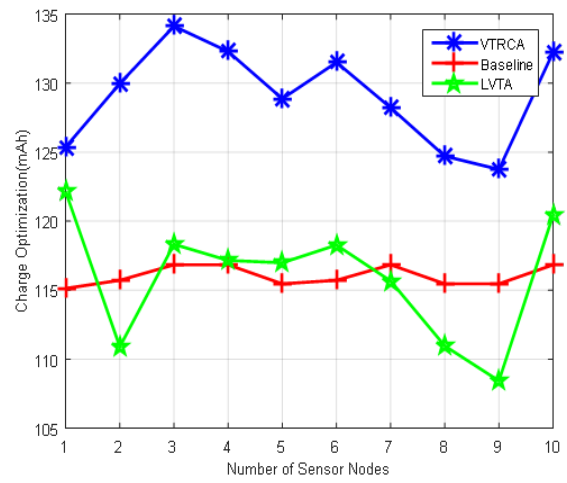
(b)



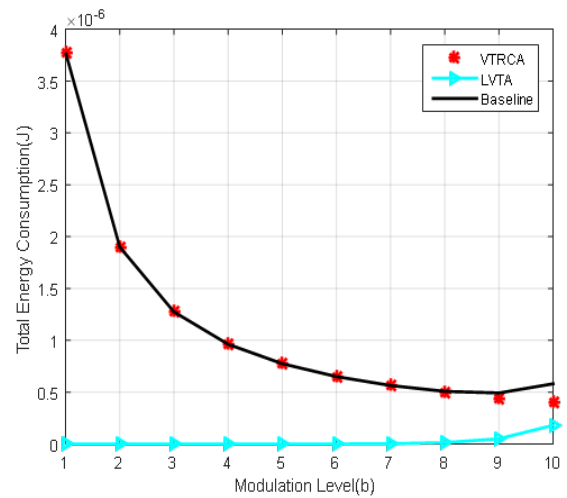
(c)



(a)



(b)



(c)

Fig. 8. QoS metrics: Time vs. a) std dev, b) PMR, c) delay vs. buffer size.

Fig. 9. a) Frame Index vs. PSNR, b) Sensor nodes vs. charge drain, c) Modulation level vs. total energy drain

to resource limited features of the small WMMDs, it is vital to fairly allocate the resources, and the overall quality of smart medical homes is based on the energy efficient communication and longer battery lifetime. The proposed VTRCA and LVTA algorithms adjust the high peak rate video frames by adopting required buffer size. Moreover, it is found that VTRCA outperforms LVTA and Baseline by saving more encoding and transmission energies while minimizing PMR and std.dev. In the near future, we will focus on quality of experience (QoE) evaluation from user's perspective in the medical IoT system domain. Despite achieving outstanding performance, there are some limitations that must be exploited by the LVTA and VTRCA algorithms. For instance, energy (i.e., encoding and transmission) depletion and delay are directly related to the buffer size.

#### ACKNOWLEDGMENT

This work is also supported by CENIIT project 17.01, Computer and Information Science department, Linköping University, Linköping, Sweden and in part by CAS President's International Fellowship Initiative Project (2020VBC0002) China

#### REFERENCES

- [1] C. Zhu, J. Tao, G. Pastor, Y. Xiao, Y. Ji, Q. Zhou, Y. Li, and A. Ylä-Jääski, "Folo: Latency and quality optimized task allocation in vehicular fog computing," *IEEE Internet of Things Journal*, vol. 6, no. 3, pp. 4150–4161, 2018.
- [2] L. Hou, L. Lei, K. Zheng, and X. Wang, "A Q-learning-based proactive caching strategy for non-safety related services in vehicular networks," *IEEE Internet of Things Journal*, vol. 6, no. 3, pp. 4512–4520, 2018.
- [3] G. Zhang, Y. Chen, Z. Shen, and L. Wang, "Distributed energy management for multiuser mobile-edge computing systems with energy harvesting devices and qos constraints," *IEEE Internet of Things Journal*, vol. 6, no. 3, pp. 4035–4048, 2018.
- [4] Y. Ye, Y. Li, G. Lu, and F. Zhou, "Improved energy detection with laplacian noise in cognitive radio," *IEEE Systems Journal*, vol. 13, no. 1, pp. 18–29, 2017.
- [5] A. Mehrabi, M. Siekkinen, and A. Ylä-Jääski, "Edge computing assisted adaptive mobile video streaming," *IEEE Transactions on Mobile Computing*, vol. 18, no. 4, pp. 787–800, 2018.
- [6] A. H. Sodhro, S. Pirbhulal, and V. H. C. de Albuquerque, "Artificial Intelligence-driven mechanism for edge computing-based industrial applications," *IEEE Transactions on Industrial Informatics*, vol. 15, no. 7, pp. 4235–4243, 2019.
- [7] S. Guo, J. Liu, Y. Yang, B. Xiao, and Z. Li, "Energy-efficient dynamic computation offloading and cooperative task scheduling in mobile cloud computing," *IEEE Transactions on Mobile Computing*, vol. 18, no. 2, pp. 319–333, 2018.
- [8] W. Zhang, Y. Sun, L. Deng, C. K. Yeo, and L. Yang, "Dynamic spectrum allocation for heterogeneous cognitive radio networks with multiple channels," *IEEE Systems Journal*, vol. 13, no. 1, pp. 53–64, 2018.
- [9] A. Venčkauskas, N. Morkevicius, K. Bagdonas, R. Damaševičius, and R. Maskeliūnas, "A lightweight protocol for secure video streaming," *Sensors*, vol. 18, no. 5, p. 1554, 2018.
- [10] C. Fan and Q. Ding, "A novel wireless visual sensor network protocol based on LoRa modulation," *International Journal of Distributed Sensor Networks*, vol. 14, no. 3, p. 1550147718765980, 2018.
- [11] C. Zhu, V. C. Leung, L. Shu, and E. C.-H. Ngai, "Green Internet of Things for smart world," *IEEE access*, vol. 3, pp. 2151–2162, 2015.
- [12] M. E. E. D. Abd El, A. A. Youssif, A. Z. Ghalwash *et al.*, "Energy aware and adaptive cross-layer scheme for video transmission over wireless sensor networks," *IEEE Sensors Journal*, vol. 16, no. 21, pp. 7792–7802, 2016.
- [13] E. Gonzalez, R. Peña, C. Vargas-Rosales, A. Avila, and D. P.-D. De Cerio, "Survey of WBSNs for pre-hospital assistance: trends to maximize the network lifetime and video transmission techniques," *Sensors*, vol. 15, no. 5, pp. 11993–12021, 2015.
- [14] L.-h. Chang, T.-C. Lin, and T.-H. Lee, "Performance analysis of video transmission over wireless multimedia sensor networks," in *International Conference on Mobile and Wireless Technology*. Springer, 2017, pp. 628–638.
- [15] "Hamlyn center laparoscopic/endoscopic video datasets," in <http://hamlyn.doc.ic.ac.uk/vision/>.
- [16] T. Mekonnen, P. Porambage, E. Harjula, and M. Ylianttila, "Energy consumption analysis of high quality multi-tier wireless multimedia sensor network," *IEEE Access*, vol. 5, pp. 15848–15858, 2017.
- [17] B. Martinez, M. Monton, I. Vilajosana, and J. D. Prades, "The power of models: Modeling power consumption for IoT devices," *IEEE Sensors Journal*, vol. 15, no. 10, pp. 5777–5789, 2015.
- [18] L. Feng, R. Q. Hu, J. Wang, and Y. Qian, "Deployment issues and performance study in a relay-assisted indoor visible light communication system," *IEEE Systems Journal*, vol. 13, no. 1, pp. 562–570, 2018.
- [19] L. Wang, L. Jiao, J. Li, J. Gedeon, and M. Mühlhäuser, "Moera: Mobility-agnostic online resource allocation for edge computing," *IEEE Transactions on Mobile Computing*, vol. 18, no. 8, pp. 1843–1856, 2018.
- [20] A. H. Sodhro, M. S. Obaidat, Q. H. Abbasi, P. Pace, S. Pirbhulal, G. Fortino, M. A. Imran, M. Qaraqe *et al.*, "Quality of service optimization in IoT-driven intelligent transportation system," *IEEE Wireless Communications*, vol. 26, no. 6, pp. 10–17, 2019.
- [21] M. Muzammal, R. Talat, A. H. Sodhro, and S. Pirbhulal, "A multi-sensor data fusion enabled ensemble approach for medical data from body sensor networks," *Information Fusion*, vol. 53, pp. 155–164, 2020.
- [22] C. Savaglio, P. Pace, G. Aloï, A. Liotta, and G. Fortino, "Lightweight reinforcement learning for energy efficient communications in wireless sensor networks," *IEEE Access*, vol. 7, pp. 29355–29364, 2019.
- [23] A. Zaidan and B. Zaidan, "A review on intelligent process for smart home applications based on IoT: coherent taxonomy, motivation, open challenges, and recommendations," *Artificial Intelligence Review*, vol. 53, no. 1, pp. 141–165, 2020.
- [24] K. E. Skouby and P. Lynggaard, "Smart home and smart city solutions enabled by 5G, IoT, AI and CoT services," in *IEEE International Conference on Contemporary Computing and Informatics (IC3I)*. IEEE, 2014, pp. 874–878.
- [25] C. Long, Y. Cao, T. Jiang, and Q. Zhang, "Edge computing framework for cooperative video processing in multimedia IoT systems," *IEEE Transactions on Multimedia*, vol. 20, no. 5, pp. 1126–1139, 2017.
- [26] C. Nykvist, M. Larsson, A. H. Sodhro, and A. Gurtov, "A lightweight portable intrusion detection communication system for auditing applications," *International Journal of Communication Systems*, vol. 33, no. 7, p. 4327, 2020.
- [27] J. Zhang, X. Hu, Z. Ning, E. C.-H. Ngai, L. Zhou, J. Wei, J. Cheng, B. Hu, and V. C. Leung, "Joint resource allocation for latency-sensitive services over mobile edge computing networks with caching," *IEEE Internet of Things Journal*, vol. 6, no. 3, pp. 4283–4294, 2018.